# EMI R&D PROJECT FINAL REPORT

All the following mandatory information needs to be provided.

| | |
|---|---|
| **Project Title:** | Understanding dynamics and impacts of cyclone systems through a comprehensive dataset of convection-permitting simulations |
| **Computer Project Account:** | spgrflao |
| **Start Year - End Year :** | 2023 - 2026 |
| **Principal Investigator(s)** | Emmanouil Flaounas |
| **Affiliation/Address:** | Hellenic Centre for Marine Research (HCMR) |
| **Other Researchers (Name/Affiliation):** | |

The following should cover the entire project duration.

## Summary of project objectives

(10 lines max)

Given the multiple scales of atmospheric processes involved in cyclone development, high-resolution simulations are irreplaceable research means to address open questions in dynamics and impacts. This project pursued a twofold objective: (i) to build a first-of-its-kind comprehensive dataset of cyclone simulations at convection-permitting scales; and (ii) to use this dataset to better understand cyclone dynamics and impacts through research projects proposed by the community, especially in the context of the MedCyclones COST Action.

## Summary of problems encountered

(If you encountered any problems of a more technical nature, please describe them here.)

The implementation of this project encountered a series of challenges, which have now been resolved to a large extent. From the technical perspective, much of the first year was devoted to the optimal configuration of the WRF model, the automation of the simulation production chain and the compilation options that make the model cost-efficient. Additional challenges concerned the post-processing of simulations, where two Lagrangian models are combined to provide air parcel trajectories for the needs of specific research projects. Storage issues were resolved by saving 3-hourly file outputs. The main remaining challenge concerned the Lagrangian post-processing: the RIP program, although adapted to the moving nested WRF domains, proved computationally slow and handles a single release time per run, which made extending trajectories into the parent domain cumbersome; this was addressed by combining RIP with the LAGRANTO model.

## Experience with the EMI R&D Project framework

(Please let us know about your experience with administrative aspects like the application procedure, progress reporting etc.)

Overall, our experience with the EMI R&D Project framework was positive. The application and reporting procedures were clear and straightforward, and access to ECMWF's high-performance computing facilities was reliable throughout the project. The allocated resources proved sufficient to complete the planned simulations.

## Summary of results

### Model setup

The simulations production chain is mainly composed by (1) the limited area model WRF, (2) the WRF pre-processing system (WPS), (3) the Read/interpolate/plot (RIP) program (a post-processing tool adapted to WRF outputs), and (4) the Lagrangian model LAGRANTO.

The operational chain for the production of simulations started with a prescribed number of cyclone tracks from ERA5, produced by the method of Flaounas et al. (2014). Each track is provided as an input to a Fortran program that produces the size and coordinates of the parent domain (at 14 km of horizontal resolution). The parent domain tightly encompasses the cyclone track. Then the program calculates the size of the nested domain (2.8 km), the directions and times of its predefined movements to always follow the cyclone centre. WPS is provided with all this information to produce the necessary input fields for WRF. The model eventually performed simulations for each cyclone track using one-way nesting. Spectral nudging is applied to the parent domain with a strength that increases linearly from the mid-troposphere to the model top at 50 hPa. Spectral nudging is necessary to force the cyclone in the parent domain not to diverge from the prescribed track from ERA5.

After the model integration is finished, we used the RIP (read/interpolate/plot) program to release 10,000 air mass trajectories every ~11 km (every 4 grid points) within the nested domain. Trajectories are released forward and backward in time for 48 hours in each time direction at 950, 850, 800, 700 and 600 hPa (so 50,000 trajectories in total per release time). If the time of maximum intensity of the cyclone (deepest MSLP according to ERA5) is set at t0, then release times are set at t0-24h, t0-12h, t0 and t0+12h. This makes a total of 4 datasets per cyclone. Each dataset includes a maximum of 50,000 trajectories where each trajectory runs for a maximum of 96 hours (we only retain trajectories that do not start below ground, and have tracked air parcels for at least 12 hours before leaving the domain). All trajectories eventually escape the nested domain. Therefore, we extend them in the parent domain using LAGRANTO backwards and forward in time for 48 hours. The change of model for the parent domain was necessary for computational reasons. Being adapted to WRF outputs, RIP takes into account that nested domains are moving in time. Nevertheless, RIP was found to have a rather slow performance and requires one release time per run. The latter issue is inconvenient when extending the trajectories in the parent domain since air parcels escape the nested domain in different times.

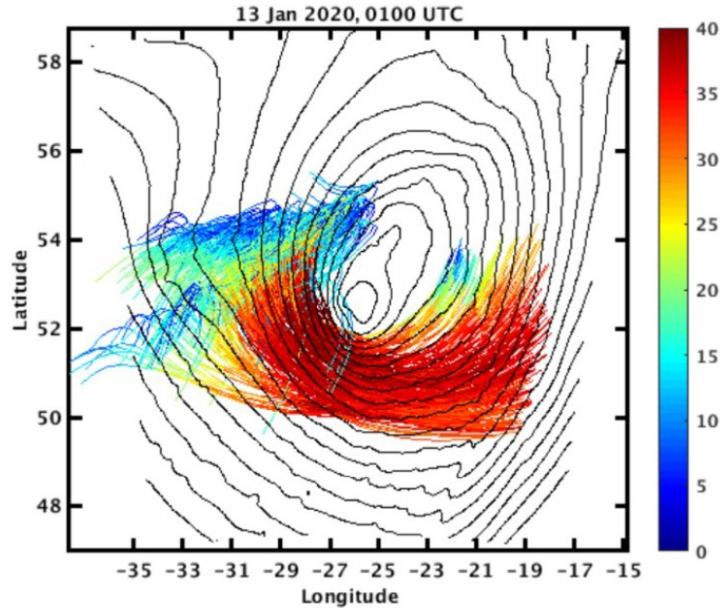


*Fig. 1: Air parcel trajectories that satisfy the condition of exceeding wind speed of 36 m s-1 below 700 hPa when they are close to the cyclone centre. We show only trajectory parts from 12 January 2020, 1900 UTC to 13 January 2020, 0700 UTC. Colorbar depicts wind speed in m s-1 and contour depicts the mean sea level pressure (cyclone centre is ~950 hPa).*

## Windstorms due to Mediterranean cyclones

In recent years, particular attention has been given to the production of results concerning high wind speeds in cyclone systems. In Volonté and Flaounas (2024), we identified specific Mediterranean storms exhibiting characteristics of extratropical cyclones that follow the Shapiro-Keyser lifecycle. For these storms, specific Lagrangian analyses were performed to identify the presence of sting jets. Our test case to verify that WRF is able to produce sting jets in cyclone systems has been done for storm Brendan (Fig. 1) that resulted in important socioeconomic impacts in the UK in January 2020. The nested WRF model domain at 2.8 km grid spacing, simulated maximum 850 hPa wind speeds exceeding 50 m/s at 03 UTC on 13 January, close to Brendan’s center and in consistency with previous results on the same storm from Gray et al. (2021; Weather). The sting jets presented a typical structure, extending from the tip of the cloud head until the edge of the frontal-fracture region. Trajectory analyses for this event revealed air parcels undergoing descent and acceleration, features consistent with the dynamic signature of a sting jet.

Out of 200 Mediterranean cyclone simulations, we could identify a small fraction of system which seemed to develop sting jets during their mature stage. For a specific case on 26 March 1998, taking place in central Mediterranean, we identified in the WRF simulation, maximum winds exceeding 30 m/s west of the warm-core low center at 03 UTC. In this instance too, threshold-meeting trajectories exhibited ascent followed by descent and acceleration—again consistent with the kinetic definition of a sting jet. The most striking case however for sting jets in the Mediterranean region has been found for the cyclone system, developing on 6 February 2012. That system exhibited the development of a bent-back front, although the overall evolution was less reminiscent of a classic warm-seclusion extratropical cyclone and despite the presence of a clear warm core (Fig. 2). The cyclone has been a rapidly deepening system (23 hPa in 18 hours) that moved northward from the Gulf of Sidra to the Ionian Sea, showing features indicative of sting jet formation. In this event, the WRF model showed indeed warm seclusion formation as the cold front advanced eastward, with strong 850 hPa winds initially appearing south of the cyclone center and while the cyclone per-se remained nearly stationary (Fig. 2). Later, the most intense winds at 850 hPa developed on the northern flank of the cyclone center where trajectories showed a circular wrapping around it, not aligning with the behavior of a typical cold conveyor belt.

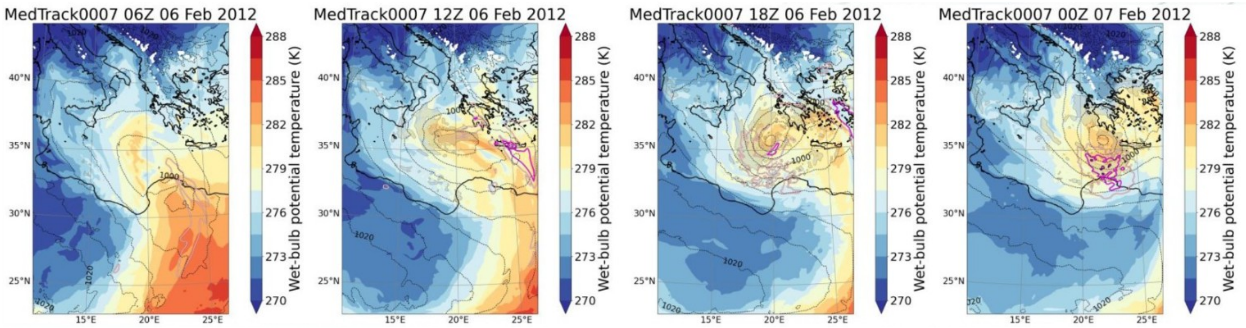


*Fig 2: Wet-bulb temperature at 850 hPa (in color) along with mean sea level pressure (in black contours) and high wind speed at 850 hPa (in magenta contours).*

Figure 3 shows air parcel trajectories associated with sting jets of the Mediterranean cyclone. These sting jets exhibit a marked descent, accompanied by increasing wind speeds and decreasing relative humidity as the parcels exit the cyclone's cloud head. These features are consistent with those expected from extratropical cyclones over the Atlantic Ocean that develop sting jets. Our results contribute to the growing evidence of "sting jet-like" airstreams associated with strong near-surface winds in convection-permitting simulations of Mediterranean cyclones. However, relevant observational data still need to be investigated to assess how realistic these model outputs are. Further analysis is also required to better understand the underlying dynamics of these airstreams and to compare or contrast them with the more typical sting jets observed in mid-latitude cyclones taking place over the open oceans. Eventually however, the key issue is not one of terminology or "labeling", but of recognizing and understanding potentially uncommon, but significant pathways through which damaging surface winds can develop in Mediterranean cyclones.

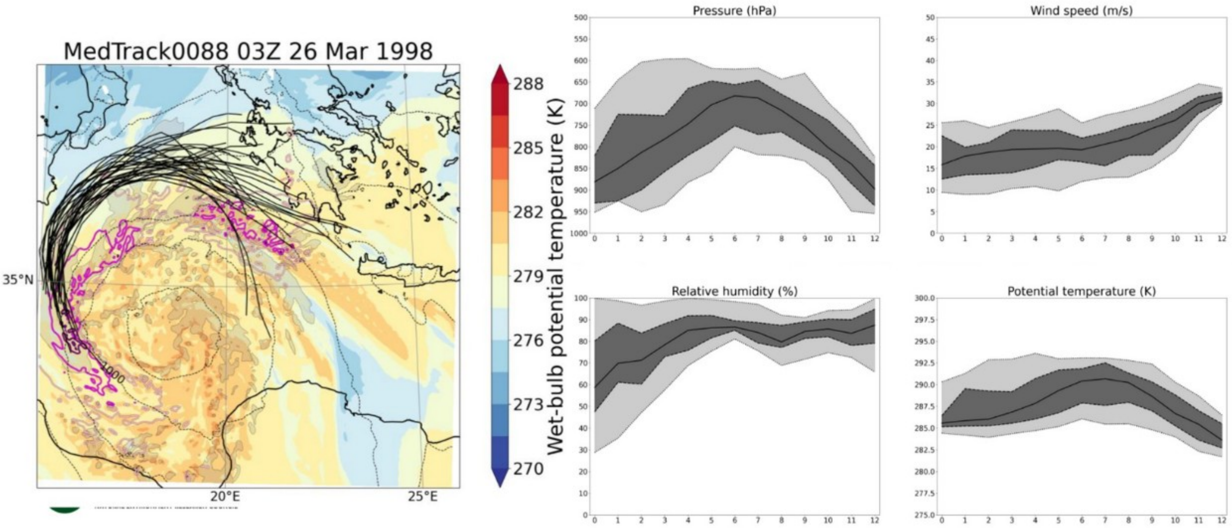


*Fig 3: (left panel) Wet-bulb temperature at 850 hPa (in color), high wind speed at 850 hPa (in magenta contours) and air parcel trajectories corresponding to sting jets. (right panel) Pressure level, relative humidity, wind speed and potential temperature of sting jet air parcels (as shown in left panel).*

In this context, the same Mediterranean cyclone has also been examined by Ferrarin et al. (2024) in the context of sea-state related impacts. In their study, the wave model SHYFEM-WW3 was forced separately with ERA5 reanalysis and the higher-resolution WRF output. During the period associated with sting jet development, a striking difference emerged between the two simulations in terms of significant wave height (Fig. 4). The WRF-forced simulation produced more realistic and substantially higher wave heights and sea levels, particularly at observation stations in Crete, compared to the ERA5-forced simulation. These findings suggest a critical sensitivity of wave modeling to atmospheric forcing resolution and are currently the subject of ongoing investigation.

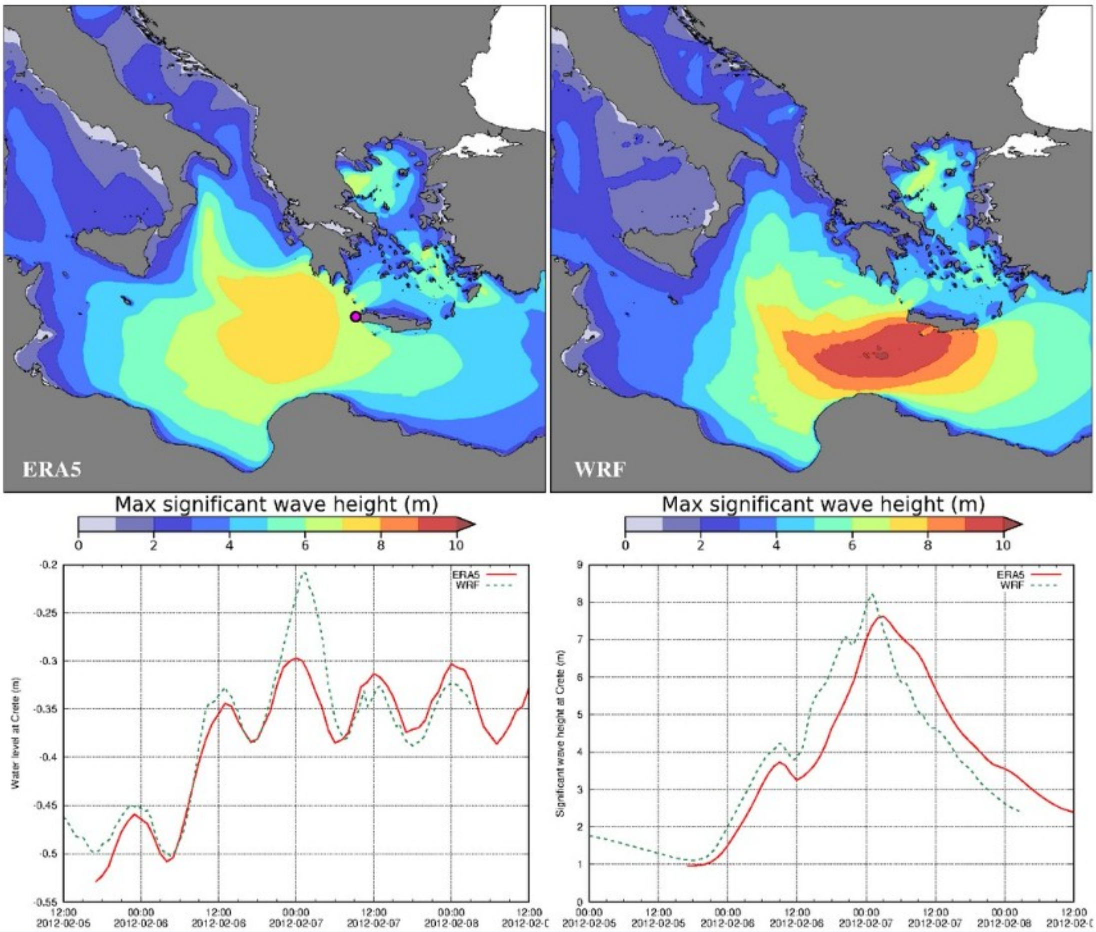


*Fig 4: (Top panels) max significant wave height on 7 Feb 2012 for SHYFEM-WW3, forced by ERA5 and WRF (in colour) along with (bottom panels) their time series at the location of western Crete.*

## Windstorms due to mid-latitude cyclones

Analysis of the simulations is still ongoing, with a particular focus on high-impact cyclones over the Atlantic Ocean and their severe consequences across Europe. About 300 simulations have been performed for cyclones over the Euro-Atlantic domain, where about 100 cyclones present sting jets. Preliminary results (Flaounas et al., 2025) highlight the significant contribution of explicitly resolved sting jets to localized wind gusts, emphasizing the value of high-resolution modeling in capturing these hazardous features. Indeed, in a recent study, we simulated the expected losses that could be caused by severe storms. To quantify the added value of our high-resolution simulations, we utilized both parent and nested model domains at 14 km and 2.8 km scales. During collaborative work with AXA, we leveraged AXA’s exposure portfolios across several European countries, including Ireland, the United Kingdom, France, Germany, and Belgium. By combining these exposure datasets with our in-house damage functions, we were able to simulate storm-related losses at the site level for each individual event. The loss model requires wind gust footprints as input—specifically, the maximum wind speeds recorded during the lifetime of each cyclone. For example, Figure 5 illustrates the wind gust footprint for Storm Eunice, which made landfall in Europe in 2022. The two simulations, at 14 km and 2.8 km resolutions, display broadly similar wind patterns with comparable peak gust magnitudes. However, the higher-resolution simulation reveals stronger wind speeds, particularly in areas impacted by a Sting Jet (highlighted in red on the left panel of Figure 5). This difference in resolution (and therefore on wind gust intensity) has a significant impact on the estimation of economic losses, resulting in an average of up to 20% relative increase among 46 intense storms which have been known about their impacts (not shown).

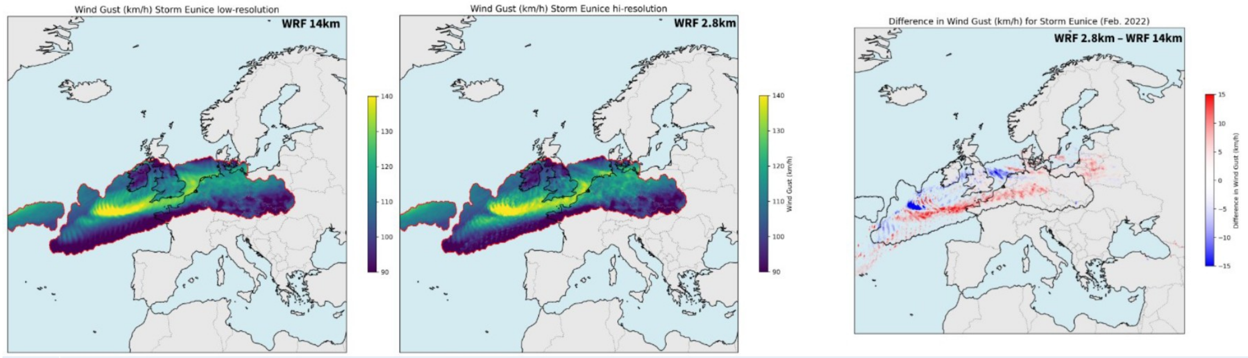


*Fig 5: (Left panels) wind gust footprint for storm Eunice (Feb 2022) from the parent and nested domain, at 14 and 2.8 km, respectively. (right panel) Difference of wind gust footprints between the two simulation domains.*

This study is still ongoing and aims at fully evaluating the added value of more accurate capturing of wind gust patterns associated with catastrophic cyclone airstreams like Sting Jets, which can significantly affect loss estimates. Our findings point to a meaningful physical footprint of sting jets in shaping windstorm damage patterns, which are often underestimated in coarser models. Furthermore, the effort to systematically explore the connection between the Atlantic and Mediterranean storm tracks is fostering valuable interdisciplinary collaboration between communities that traditionally have had limited interactions so far.

## Sting jets climatology

In total, we identified 100 cyclones associated with sting jets. These cyclones were drawn from a special subset of simulations derived from Gray et al. (2023), who used an explicit identification method that qualified cyclones from ERA5 as potential sting jet precursors. We additionally identified a list of cyclones whose air mass trajectories were relevant to sting jets: they presented maximum wind speeds exceeding 30 m $s^{-1}$ below 800 hPa and, within a time window of 12 hours prior to their maximum wind speed, exhibited relative humidity above 70% while being located at least 100 hPa higher. Figure 6 shows a composite analysis of all air parcel trajectories identified as sting jets. Boxplots show the distribution of atmospheric variables at times relevant to the onset of descent of the air parcel trajectories. For all cases, the pattern is remarkably close to what has been identified in individual case studies; nevertheless, this is the first time a statistical perspective is presented that comprises an ensemble of cases. This is particularly challenging, since sting jet development requires high-resolution modelling, whereas not all cyclones — even those presenting the mesoscale characteristics that would potentially allow such development — are eventually able to exhibit these features.

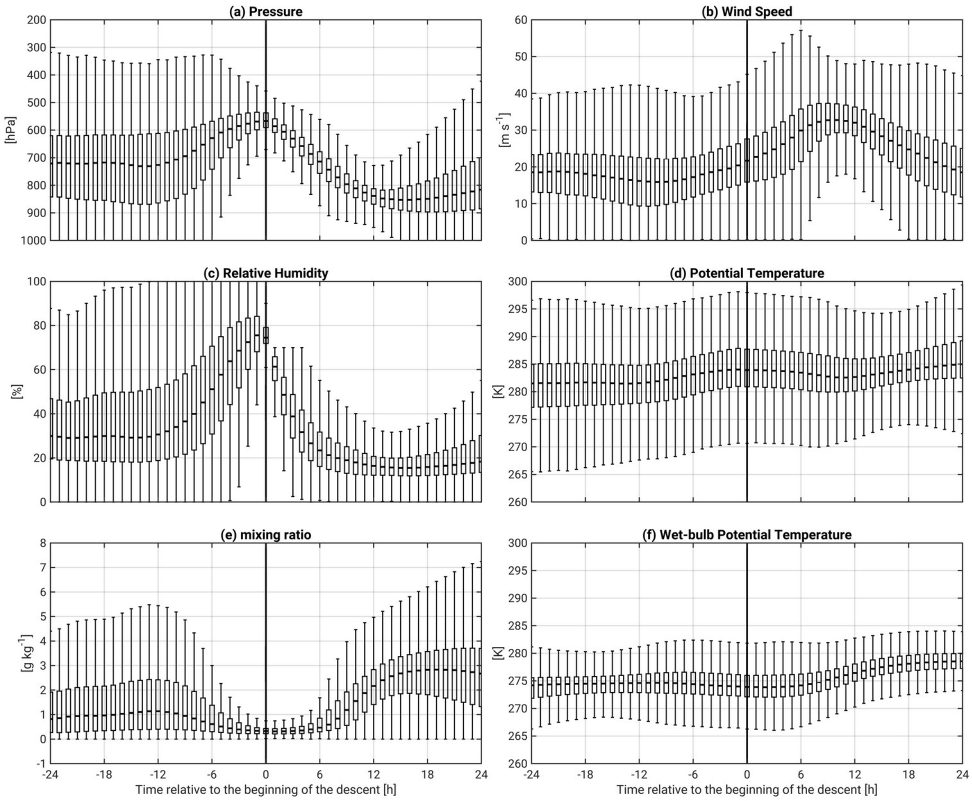


*Fig 6: Sting jet air parcel trajectories showing (a) pressure evolution, (b) wind speed, (c) relative humidity, (d) potential temperature, (e) mixing ratio and (f) wet-bulb potential temperature.*

It is interesting to stress that, out of the ensemble of 100 cyclone cases, a few did not comply with the cyclone structure expected to allow sting jet development, namely the formation of a warm seclusion and the associated instabilities. In this respect, it is the first time we explicitly identify sting jet air parcel trajectories associated with cyclones that are not of the classical type usually linked to these airstreams. Figs 7 and 8 show two such cyclone cases, where air parcels (blue dots) are clearly located within the cloud head of the cyclone (Figs 7a and 8a) and, within a time window of less than 12 hours, descend into a region of high wind speed ahead of the cyclone (Figs 7b and 8b; blue contour). Figures 7c, 7d, 8c and 8d show the 2-metre temperature field, making clear that these cyclones, in contrast to typical cases, are not associated with a clear warm seclusion — the life cycle that would normally accompany sting jet development. These two cases offer a rather different perspective on sting jet air parcels, one that can only be revealed through high-resolution physical simulations. A paper presenting this climatology together with these two non-classical cases is currently in preparation.

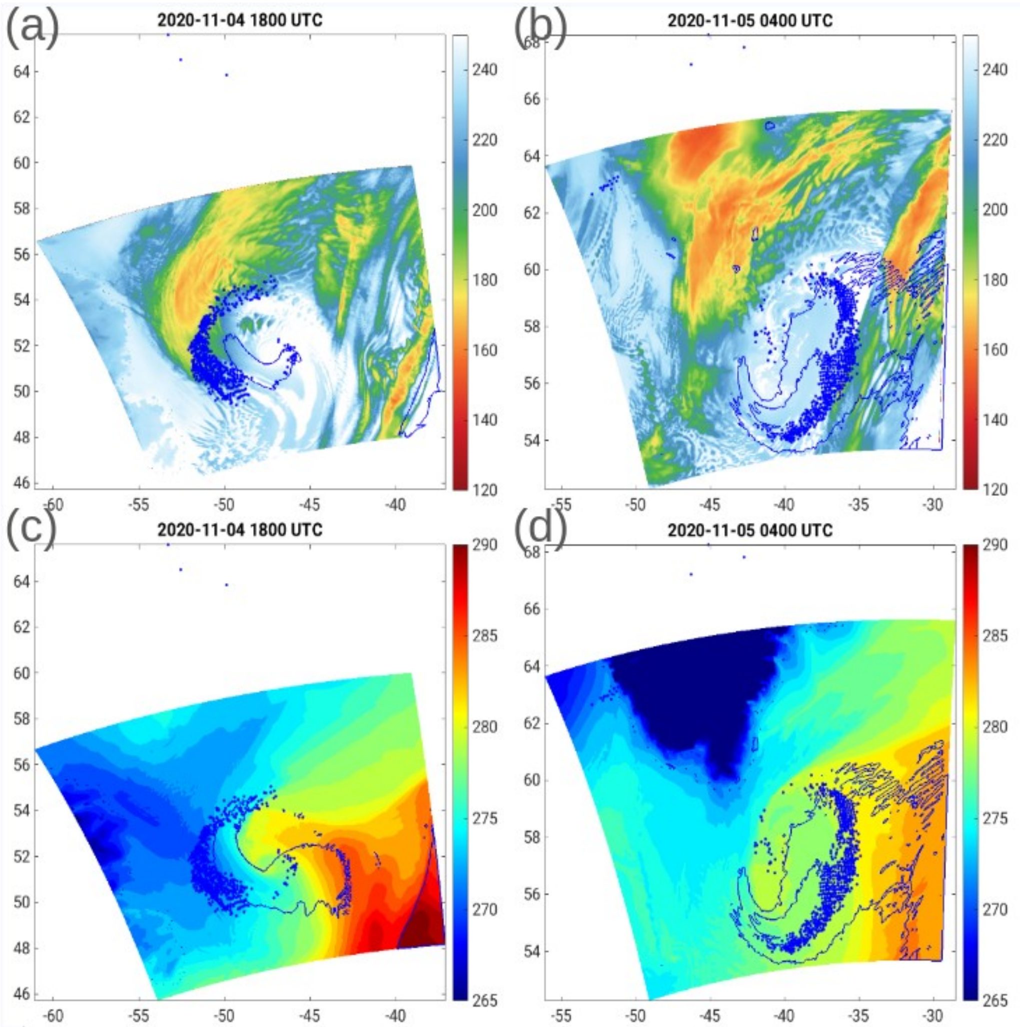


*Fig 7: Cyclone case of November 2020. (a) Outgoing longwave radiation (in colour), area of surface wind gusts exceeding 20 and 25 m s⁻¹ (two blue contours), and location of air parcels before starting their descent (blue dots) at time 0h in Fig. 6; (b) same as in (a) but at time of maximum wind speed of air parcels (roughly at time +10h in Fig. 6); (c) same time and fields as (a) except that coloured shading shows temperature at 2 metres; (d) as in (c) but for the same time as (b).*

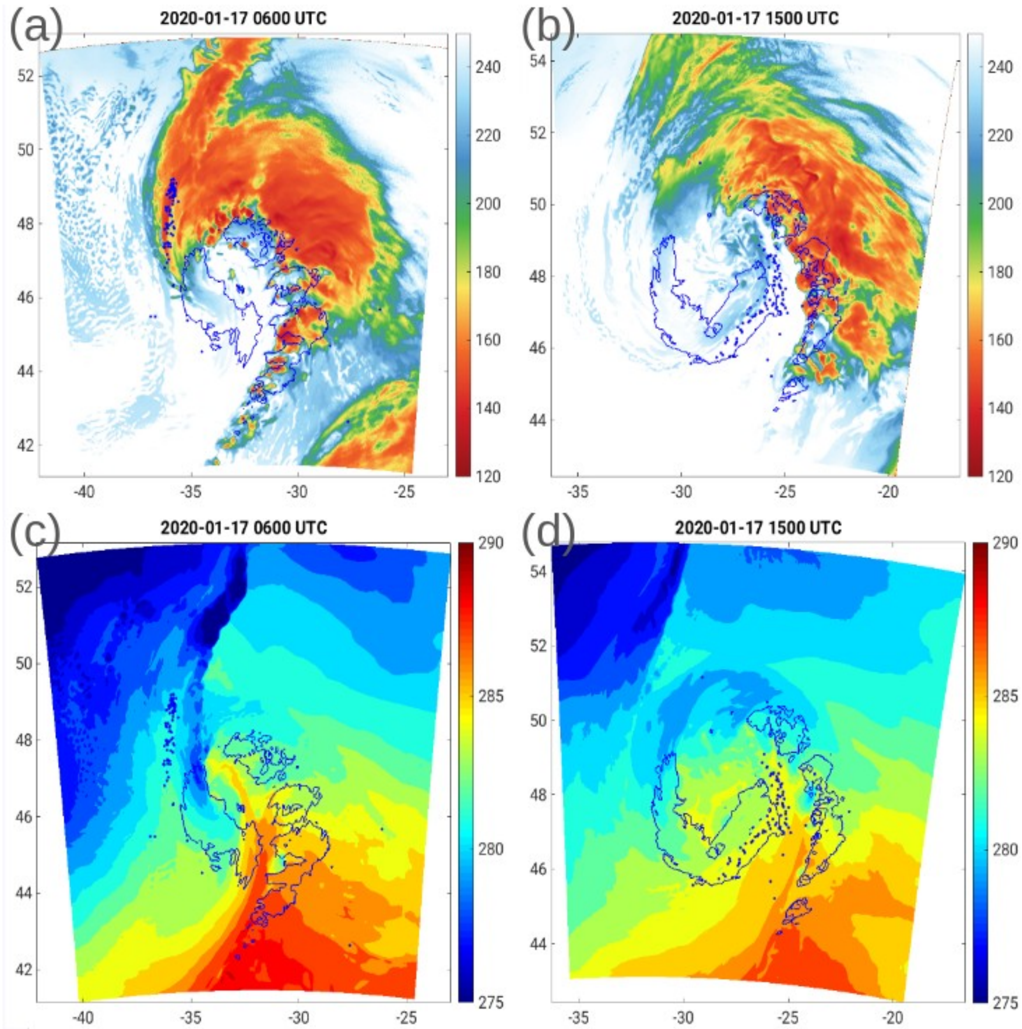


*Fig 8: As in Fig. 7 but for the cyclone case of January 2020.*

## List of publications/reports from the project with complete references

Hatzaki, M., and Coauthors, 2023: MedCyclones: Working Together toward Understanding Mediterranean Cyclones. Bull. Amer. Meteor. Soc., 104, E480–E487, https://doi.org/10.1175/BAMS-D-22-0280.1.

Volonté, A., and E. Flaounas, 2024: Sting jets in Mediterranean cyclones? Working towards their identification using high-resolution simulations. 3rd MedCyclones Workshop & Training School, 15–19 July 2024, ESA-ESRIN, Frascati (Rome), Italy.

Ferrarin, C., M. Bajo, and E. Flaounas, 2024: The marine and coastal hazards of Mediterranean cyclones. 3rd MedCyclones Workshop & Training School, 15–19 July 2024, ESA-ESRIN, Frascati (Rome), Italy.

## Future plans

With the simulation dataset now essentially complete (about 200 Mediterranean and 400 North Atlantic convection-permitting cases), the immediate priority is to finalise the Lagrangian post-processing and to make the dataset openly available to the community. In addition, we need to finalise ongoing analyses, including the sting jet climatology described above and the associated non-classical cyclone cases which are being prepared for peer-reviewed publication.